

Compact Tri-Band Patch Antenna for Ku Band Applications

Rajeev Kumar^{1,*}, Gurpreet Singh Saini², and Daljeet Singh²

Abstract—A compact tri-band antenna is designed and analyzed to achieve both transmission and reception of direct broadcast service (DBS) and fixed satellite service (FSS) in Ku band. The proposed antenna design consists of a truncated E-shaped slot, eight rectangular slots, two C-shaped slots in the patch and eight defected ground structure (DGS) slots. The three frequency bands of 11.40–12.91 GHz, 13.86–14.53 GHz, and 17.20–17.86 GHz are achieved with impedance bandwidths of 12.32%, 4.73%, and 3.77%, respectively. Conversely, the measured frequency bands of 11.40–12.98 GHz, 14.21–14.86 GHz, and 17.41–18.98 GHz with the impedance bandwidth of 12.70%, 4.48%, and 8.63%, respectively, are obtained. The simulated results of the proposed antenna are compared with the results of fabricated antenna and are found to be satisfactory for reflection coefficient, impedance bandwidth, polarization, efficiency, gain, and radiation pattern. Moreover, the proposed antenna design can be used as an element in an array configuration to achieve high gain in both transmission and reception modes of FSS and DBS.

1. INTRODUCTION

With the developments in satellite technology, the use of satellite antenna in various applications like cellular communication, weather forecasting, TV broadcasting, navigation, monitoring, surveillance, etc. has exponentially increased. At earth station, generally, a bulky and large parabolic reflector antenna is used for this task. Such an antenna is not desirable due to space and environmental constraints. Also, the radio is not static in one position in most of the satellite applications. Therefore, a low profile patch antenna is utilized for multi-band performance, miniature dimensions, robustness against interference, and cheap fabrication budget [1].

Conventionally, the antennas used in such applications are single-band antennas, i.e., operating at a single frequency. However, due to the proliferation in a number of possible applications originating in a single system and space constraints, multiband antennas have become a strong candidate for present and future Ku-band satellite communication systems [2]. In the literature, many antennas have been proposed to fulfill the requirement of multiband applications [1–3]. A lot of patch antennas have been designed for Ku-band satellite applications such as dual-band antenna with single-layer and single-patch for Ku-band satellite application, low profile patch antenna, and loaded slot patch antenna for applications in Ku-band [4–10].

Fixed satellite services (FSS) and direct broadcast services (DBS) are two important applications of satellite communication that are governed by the International Telecommunication Union (ITU). For this task, ITU has divided the globe into three regions. For region 3, the frequency band requirements for FSS are: 14–14.5 GHz (transmission) and 12.2–12.7 GHz (reception) and for DBS are 17.3 GHz–17.8 GHz (transmission) and 11.7 GHz–12.2 GHz (reception).

Received 31 January 2020, Accepted 4 June 2020, Scheduled 17 June 2020

* Corresponding author: Rajeev Kumar (rajeev.kumar@chitkara.edu.in).

¹ Chitkara University Institute of Engineering and Technology, Chitkara University, Punjab, India. ² School of Electronics and Electrical Engineering, Lovely Professional University, Phagwara, Punjab, India.

Researchers around the world have worked on design, fabrication, and optimization of antennas for FSS and DBS according to ITU norms. In [11], a dual-band antenna with 3.4–3.6 GHz and 5.725–5.825 GHz for 5G and 5.8G Wi-Fi are achieved, respectively. A Spidron-Fractal antenna operating in the Ku band of 11.44–12.48 GHz and 13.47–14.39 GHz is proposed by Nguyen Thi et al. in [12]. In [13], a triple-band parasitic array antenna is designed in order to optimize the total inductance of geometry for achieving C, X, and Ku bands. Mathew et al. [14] present a tri-band antenna using a circular disc sector for UMTS, WiMAX, and ISM band applications.

In [15], an X-shaped patch antenna containing five rectangular slots is presented. The design is proposed for frequency ranges of 15.104–15.632 GHz, 17.336–17.912 GHz, and 18.476–19.280 GHz. Naghar et al. in [16] propose an antenna for C (4.9–7 GHz), X (7.92–11.08 GHz), and Ku (11.85–15.94 GHz) bands. This design comprises a modified rectangular element with U-shaped slots along with deformed ground plane. In [17], the authors propose a C, X, and Ku band hexagonal patch microstrip antenna using an FR4 substrate. Partial ground planes along with unsymmetrical slots are used in the design.

In [18], a defected patch and ground-based antenna is proposed for 15.27–16.51 GHz. A defected ground structure (DGS) based fractal antenna design is studied in [19]. The frequency range of operation is given to be 1–7 GHz. In [21], a three-dimensional meandering probes based antenna is proposed for Ku band. The technology of a multilayer printed circuit board is utilized in [21]. Deng et al. [22] propose a reflectarray (RA) type antenna for Ku band applications. An aperture efficiency of 60% is measured for the frequency bands of 12.0–14.9 GHz. Huang et al. [23] propose a planar patch antenna array having circular polarization. The proposed antenna is claimed to have a bandwidth of 700 MHz from 11.55 to 12.25 GHz (Ku band). In [24], a $25 \times 30 \text{ mm}^2$ hexagonal-triangular fractal antenna is designed for 3–25.2 GHz. Using this design, a gain of 3–9.8 dBi has been achieved [24]. The Ku band for FSS transmission and reception as well as DBS reception is achieved for region 3 by [4]. The authors in [4] claim that the dual bands with impedance bandwidths of 10% and 8% are achieved for lower band and upper band, respectively. Recently, in [7], the bands 11.69–13.24 GHz and 13.72–15.07 GHz are achieved by a patch antenna.

To summarize, only a few antenna designs are proposed for FSS and DBS to achieve both transmission and reception completely. Moreover, most of the designs for this purpose utilize multi-patch, multi-layered, aperture coupled, or proximity coupled structures. Practical implementation of these structures is very difficult because they face alignment issues and the air gap between layers. Further, the height and weight of these antennas (Multi-layered design with co-axial cable) are more than the patch antenna. It is incompatible to use as a conformal surface antenna. In order to achieve this target, a tri-band antenna is analyzed which covers the frequency band for both transmission and reception of DBS and FSS in Ku band and is compact in size. The design consists of truncated E-slots, C-shaped slots, and defected ground structure (DGS) slots. The fabricated antenna results are compared with the simulated ones obtained from the proposed design and are found satisfactory for the radiation pattern, impedance bandwidth, polarization, efficiency, gain, and reflection coefficient. Moreover, the proposed design can be used as an element in an array configuration to achieve high gain in both transmission and reception modes of FSS and DBS. This gain can be further enhanced using more refined and costly material like RT Duroid substrate. The remaining paper is organized as follows. The details about proposed antenna design are described in Section 2. Section 3 presents the parametric analysis of antenna design. The simulated and measured results with extensive discussions are presented in Section 4. Section 5 concludes the paper.

2. PROPOSED ANTENNA DESIGN

The geometrical design of the proposed antenna is shown in Fig. 1 and Fig. 2. Fig. 1(a) shows the front view of E slot, and the zoomed view of E slot is shown in Fig. 1(b). Fig. 2 presents the back view of the proposed antenna. The description of dimensions (mm) of the proposed antenna is listed in Table 1. The total dimensions of proposed design are $20 \times 20 \text{ mm}^2$. The design is constructed with a 1.6 mm thick (h_1) FR-4 substrate due to its cost-effectiveness. The dielectric loss tangent and relative permittivity of used FR-4 are 0.025 and 4.3, respectively. The software tool used for simulation of the antenna design is Ansys HFSS.

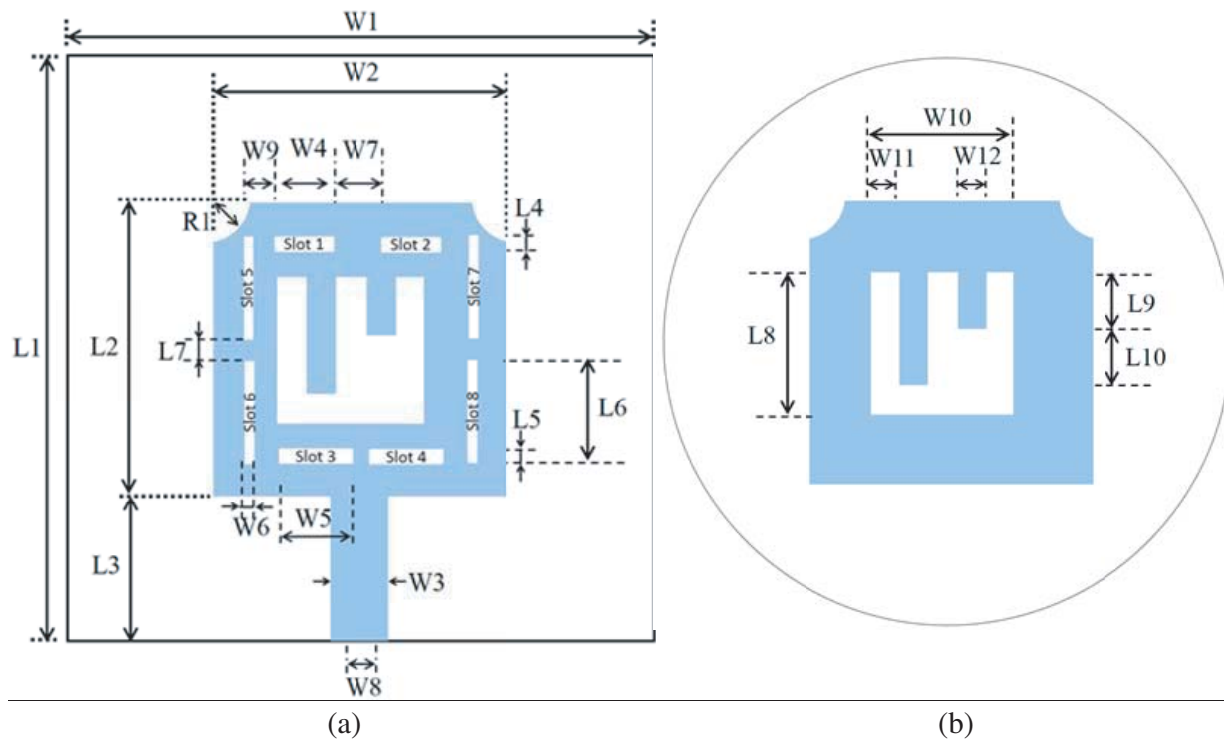


Figure 1. Proposed antenna design: (a) Front view and (b) zoomed view of E slot.

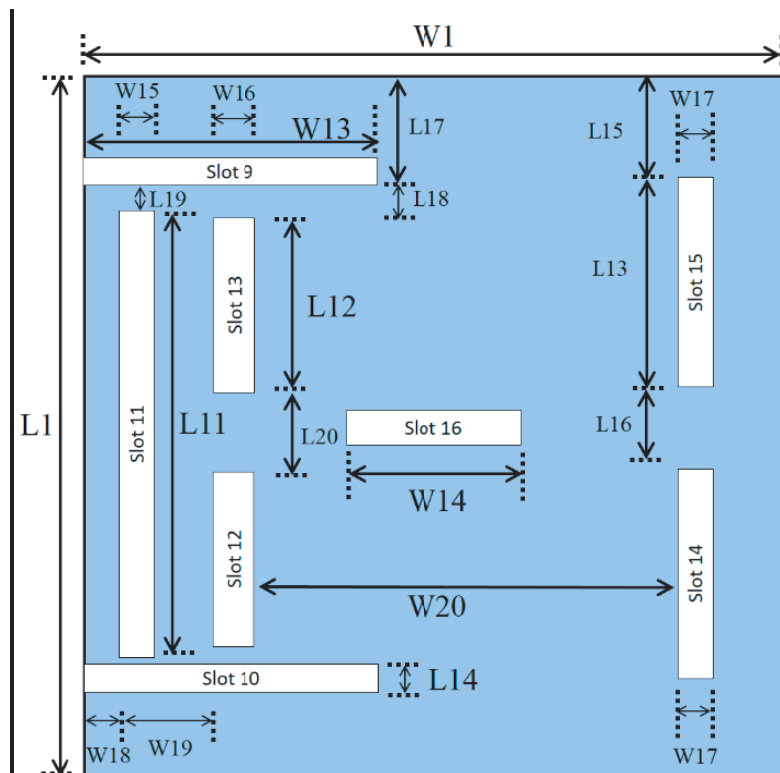


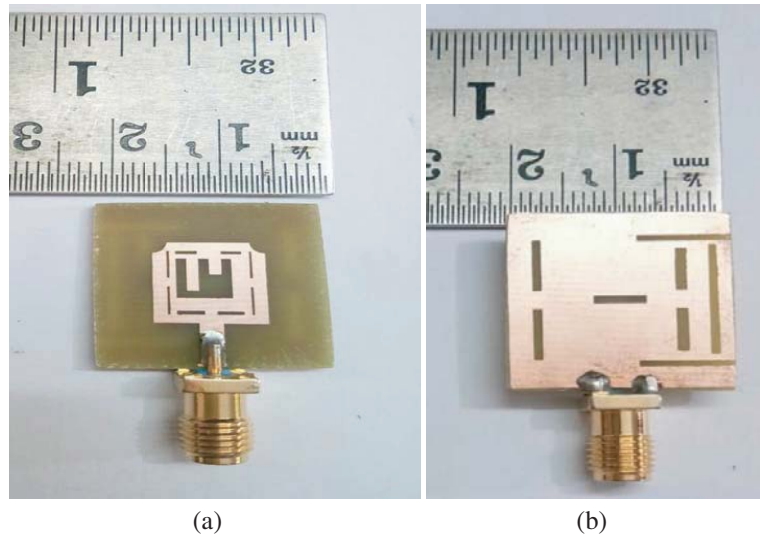
Figure 2. Proposed antenna design: Back view.

Table 1. Dimensions (in mm) of proposed design.

Length	Dimension	Width	Dimension	Length	Dimension	Width	Dimension
L_1	20	W_1	20	L_{11}	12.8	W_{12}	1
L_2	10	W_2	10	L_{12}	5	W_{13}	8.4
L_3	5	W_3	2	L_{13}	6	W_{14}	5
L_4	0.5	W_4	2	L_{14}	0.8	W_{15}	1
L_5	0.5	W_5	2.5	L_{15}	3	W_{16}	1.2
L_6	3.5	W_6	0.3	L_{16}	2	W_{17}	1
L_7	1	W_7	2	L_{17}	3	W_{18}	1
L_8	5	W_8	1	L_{18}	1	W_{19}	2.8
L_9	2	W_9	0.5	L_{19}	0.6	W_{20}	12
L_{10}	2	W_{10}	5	L_{20}	2	H_1	1.6
R_1	1.3	W_{11}	1				

Patch antenna acts as a resonant cavity; therefore, multimodes are present with different cut-off frequencies. But in the proposed design, the direction of E-field is towards the y plane. So, length of the design is selected to transmit $\text{TM}_{0\delta}$ along with dominant mode TM_{01} , where the range of δ is from 1 to 3. In this mode, there is a half-wave change along the y -axis while there are no changes along the x -axis. Higher modes above the range of δ are not desirable since they have a higher loss, and the field pattern may change over the transmission.

Initially in the proposed design, a truncated E-shaped slot is etched from the patch which gives the frequency bands of 12.08 to 13.20 GHz and 13.96 to 15.05 GHz with a resonant frequency of 12.65 GHz and 14.5 GHz, respectively. For finer tuning, eight rectangular slots are used to attain the bands of 11.7 GHz to 12.7 GHz and 14 to 14.5 GHz. The patch design is further modified with two C-shaped corner truncated slots in order to achieve transmitting and receiving modes of DBS. As a consequence, the third band of 16.93–17.5 GHz is achieved by this step. However, this band requires finer tuning as the actual band for DBS transmission is 17.3–17.8 GHz. Therefore, eight DGS slots are used in the design to achieve all the bands of FSS and DBS (transmission and reception) with enhanced bandwidth. Fig. 3 gives the final fabricated design of antenna.

**Figure 3.** Fabricated antenna ($20 \times 20 \text{ mm}^2$). (a) Front view. (b) Back view.

The simulated surface current distribution of proposed design can be visualized from Fig. 4. Figs. 4(a) and 4(b) give the current distribution for 12.25 GHz, whereas 4(c) and 4(d) are for 14.16 GHz; 4(e) to 4(f) are for 17.50 GHz. The rainbow color spectrum shows the intensity of current in

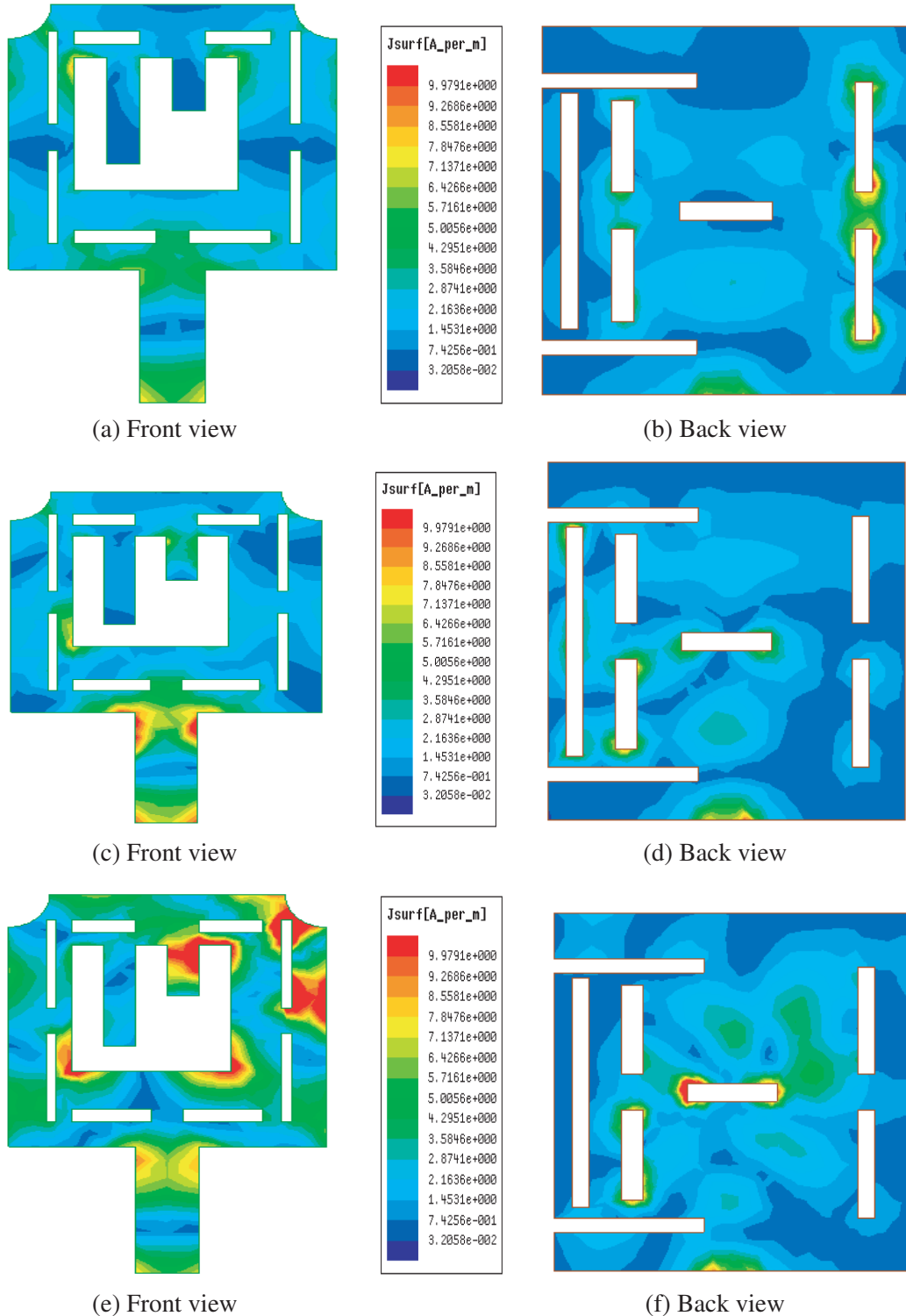


Figure 4. Distribution of current across the proposed design at (a), (b) 12.25 GHz, (c), (d) 14.16 GHz, and (e), (f) 17.50 GHz.

ampere/meter. Figs. 4(a), 4(c) and 4(e) show the surface current distribution for the top view of the patch with truncated E-shaped slot, slots 1–8, and truncated corners conversely; Figs. 4(b), 4(d), and 4(f) show the surface current distributions for the ground plane with slots 9 to 16 for clear understanding. By analyzing Figs. 4(a) and 4(b), it has been observed that the first resonant frequency of 12.25 GHz is mainly due to the current concentration on the upper part of the E-shaped slot, slot 3 to slot 5, slot 12 to slot 15. From Figs. 4(c) and 4(d), it has been noticed that the resonant frequency of 14.16 GHz is mainly due to the current concentration on the lower part of E-slot, left corner of the patch, slot 3, slot 4, slot 11, slot 12, and slot 16. Further, the current concentration on the E-slot, slot 7, slot 12, and slot 16, Figs. 4(e) and 4(f), are responsible for 17.50 GHz.

3. PARAMETRIC ANALYSIS

The following general equations have been utilized in order to compute the preliminary measurements of design. The proposed design starts with operating frequency f_1 , required permittivity ε_r , and substrate thickness h_1 . Based on the transmission line model, length L_1 and width W_1 of the patch are calculated as [25–27]:

$$\Delta L = 0.412 \frac{(\varepsilon_{ref} + 0.3) \left(\frac{W_1}{h_1} + 0.264 \right)}{(\varepsilon_{ref} - 0.258) \left(\frac{W_1}{h_1} + 0.8 \right)} h_1 \quad (1)$$

The effective length of the patch becomes

$$L_1 = L_{eff} - 2\Delta L \quad (2)$$

The effective length (L_{eff}), for resonant frequency (f_1), is given as

$$L_{eff} = \frac{c}{2f_1\sqrt{\varepsilon_{ref}}} \quad (3)$$

and

$$\varepsilon_{eff} = \frac{\varepsilon_r + 1}{2} + \frac{\varepsilon_r - 1}{2} \left[1 + 12 \frac{h_1}{W_1} \right]^{-\frac{1}{2}} \quad (4)$$

The resonance frequency corresponds to any TM_{mn} mode is given as

$$f_1 = \frac{c}{2\sqrt{\varepsilon_{ref}}} \left[\left(\frac{m}{L_1} \right)^2 + \left(\frac{n}{W_1} \right)^2 \right]^{\frac{1}{2}} \quad (5)$$

Here, m and n are modes with respect to L_1 and W_1 , respectively. For resonance, the width is given as:

$$W_1 = \frac{c}{2f_1\sqrt{\frac{\varepsilon_r + 1}{2}}} \quad (6)$$

$L_1 \times W_1$ are $10 \times 10 \text{ mm}^2$ which is $\lambda_0/2 \times \lambda_0/2 \text{ mm}^2$ where λ_0 is the center wavelength. Initially, we have obtained frequency bands with central frequencies 13.85 and 15.55 GHz. This square patch is modified with a symmetric E-shaped slot centered at the origin and results in a shift in resonant frequency to 13.2 GHz and 15.6 GHz, which can be used for transmitting and receiving modes of fixed satellite services. It has been observed that there is a minor shift in upper resonant frequency. Therefore, the E-shaped slot is truncated to achieve resonant frequency at 12.65 GHz and 14.5 GHz. This results in a significant change in upper resonant frequency. However, unfortunately, the introduction of the E slot requires fine-tuning in bandwidth which is thereafter enhanced using eight rectangular slots on the patch of antenna design.

The insertion of slots 1–4 results in minor shift of resonant frequency to 12.8 GHz and 14.5 GHz. Finally, fine-tuning is done by inserting slots 5–8 into the proposed structure in order to achieve dual-frequency peaks at 12.5 GHz and 14.1 GHz. The result of reflection coefficient (S_{11}) v/s frequency with

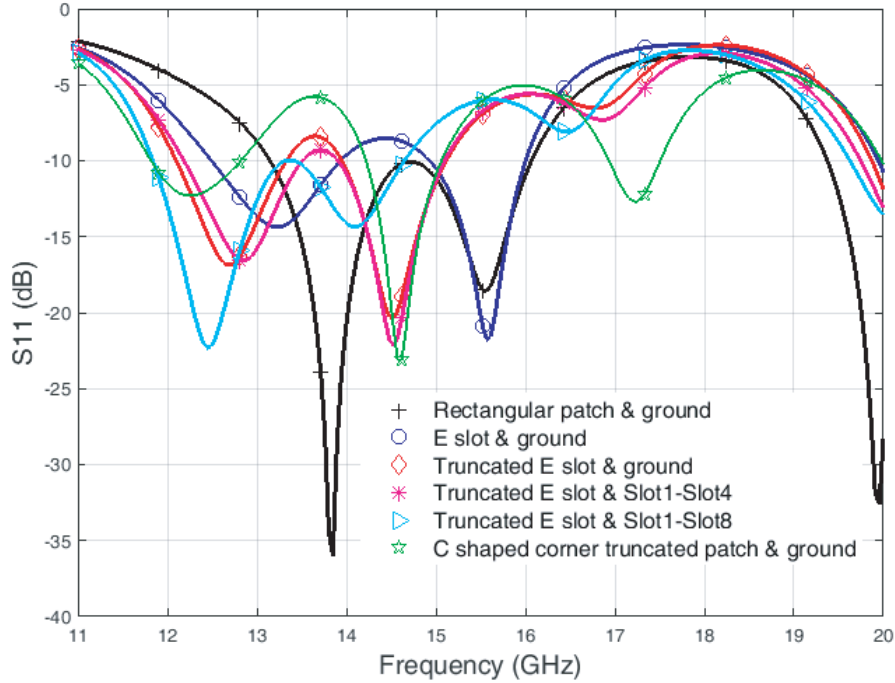


Figure 5. Reflection Co-efficient (S_{11} (dB)) v/s frequency (GHz) with E-Slot, Truncated E slot, Slot 1–Slot 8 and C shaped truncated patch and ground.

different configurations of proposed antenna design like with rectangular patch and ground, E slot and ground, truncated E slot and ground, truncated E slot with slots 1–4, and truncated E slot with slot 4–8 are given in Fig. 5. The fact that two bands are achieved with truncated E slot and slot 1 to slot 8 can be visualized from Fig. 5.

Further, in order to achieve transmitting and receiving modes of DBS, antenna design is modified with C-shaped corner truncated slots. As a consequence, three bands of 11.84–12.79 GHz, 14.19–15.05 GHz, and 16.93–17.5 GHz are now achieved, and results are shown in Fig. 5. The first band is found to be very close to DBS receive mode frequency (11.7 GHz–12.2 GHz). Also, the third band is close to DBS transmitting mode frequency (17.3 GHz–17.8 GHz).

Lastly, in order to achieve desired DBS bands, defected ground structure (DGS) technique is utilized. Slots 9, 10, and 11 are introduced in the ground plane resulting in the generation of desired DBS receive band but with very poor S_{11} . To overcome these problems, slots 12, 13, 14, and 15 are introduced. Finally, with slot 16, the exact desired bands, i.e., transmitting and receiving modes of DBS and FSS with better S_{11} and enhanced bandwidth have been achieved. The plots of S_{11} (dB) as a function of frequency for the cases of a C-shaped corner truncated patch with the ground, DGS with slots 9–10, DGS with slot 11, DGS with slots 12–13, DGS with slots 14–15, and finally DGS with slot 16 are shown in Fig. 6.

4. RESULTS AND DISCUSSION

The results obtained from simulation are presented and compared with results of the hardware prototype of the proposed design. For simulation, High Frequency Structure Simulator (HFSS) is utilized to enhance different parameters of the antenna. The effect of changing different slot dimensions on the performance of antenna is studied by varying dimensions of one slot and keeping all other slot dimensions constant. This results in the allocation of optimal dimensions for a superlative performance of the proposed design.

Figure 7 shows the S_{11} v/s frequency plots for both simulated and measured results. Observations from Fig. 7 conclude that the proposed design works satisfactorily for the bands 11.40–12.91 GHz,

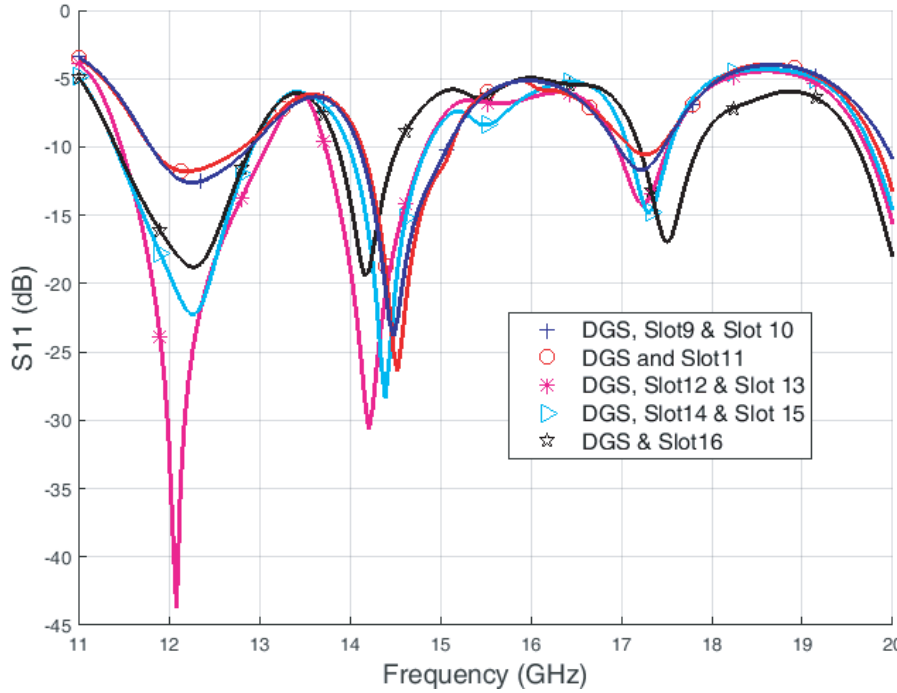


Figure 6. Reflection Co-efficient (S_{11} (dB)) v/s frequency (GHz) with DGS and Slot 9–Slot 16.

13.86–14.53 GHz, and 17.20–17.86 GHz formally introduced by ITU for transmission and reception of DBS and FSS. Another important observation can be made from Fig. 7 that the simulation results are in accordance with measured results except in a few instances. The reason behind this ambiguity may be the fabrication loss, connector loss, and tolerance in dielectric constant. Further, the dependency of dielectric constant (ϵ_r) on operational frequency is also a key factor that generally decreases with an increase in frequency. The numerical values of three frequency bands obtained by simulated and measured results are given in Table 2. Lower frequency (LF), upper frequency (UF), resonant frequency (RF), and bandwidth (BW) are taken as parameters for Table 2.

Table 2. Simulated and measured results of first, second and third band for DBS and FSS.

Frequency band (GHz)	Simulated Results				Measured Results			
	LF	UF	RF	BW	LF	UF	RF	BW
First band	11.40	12.91	12.25	1.51	11.40	12.98	12.44	1.58
Second band	13.86	14.53	14.16	0.67	14.21	14.86	14.5	0.65
Third band	17.20	17.86	17.50	0.66	17.41	18.98	18.18	1.57

The measured results are calculated using the setup given in Fig. 8. Measurements are performed inside an anechoic chamber situated in the research lab of Indian Institute of Technology (IIT), Roorkee, India. Fig. 9 presents the radiation pattern of co- and cross-polarizations. The frequencies of 12.25 GHz, 14.16 GHz, and 17.50 GHz are taken for observation in Fig. 9 for both simulated and measured results. It can be noticed from Fig. 9 that the radiation patterns of co-polarization have comparatively higher values than the cross-polarization. Therefore, it can be noted that the radiation pattern of the proposed antenna is almost broadside. For further improvement in radiation efficiency, a substrate with low dielectric losses can be utilized. The slight difference between simulated and measured results of Fig. 9 may be due to high mode excitation, the losses due to the cable/connector, the manual positioning, etc.

Figure 10 shows the plot of simulated and measured results for gain v/s frequency. The simulated

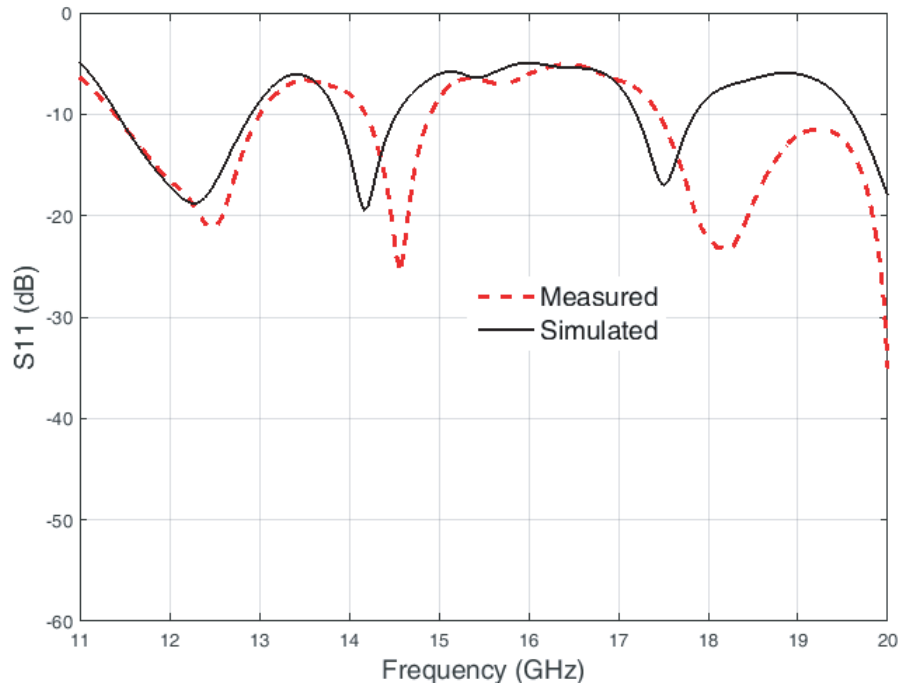


Figure 7. Simulated and measured results of S_{11} v/s frequency for the proposed design.



Figure 8. Measurement setup for the proposed antenna.

values of gain vary from 3.18 to 6 dBi, 2.08 to 4 dBi, and 2.10 to 3.70 dBi at the frequency bands 11.40–12.98 GHz, 14.21–14.86 GHz, and 17.41–18.98 GHz, respectively. On the other hand, the measured gain varies from 2.78 to 5.76 dBi, 1.70 to 3.48 dBi, and 1.10 to 3.05 dBi at the frequency bands 11.40–12.98 GHz, 14.21–14.86 GHz, and 17.41–18.98 GHz, respectively. For every reading, the Vector Network Analyzer (VNA) was recalibrated in order to further enhance the precision of measured results.

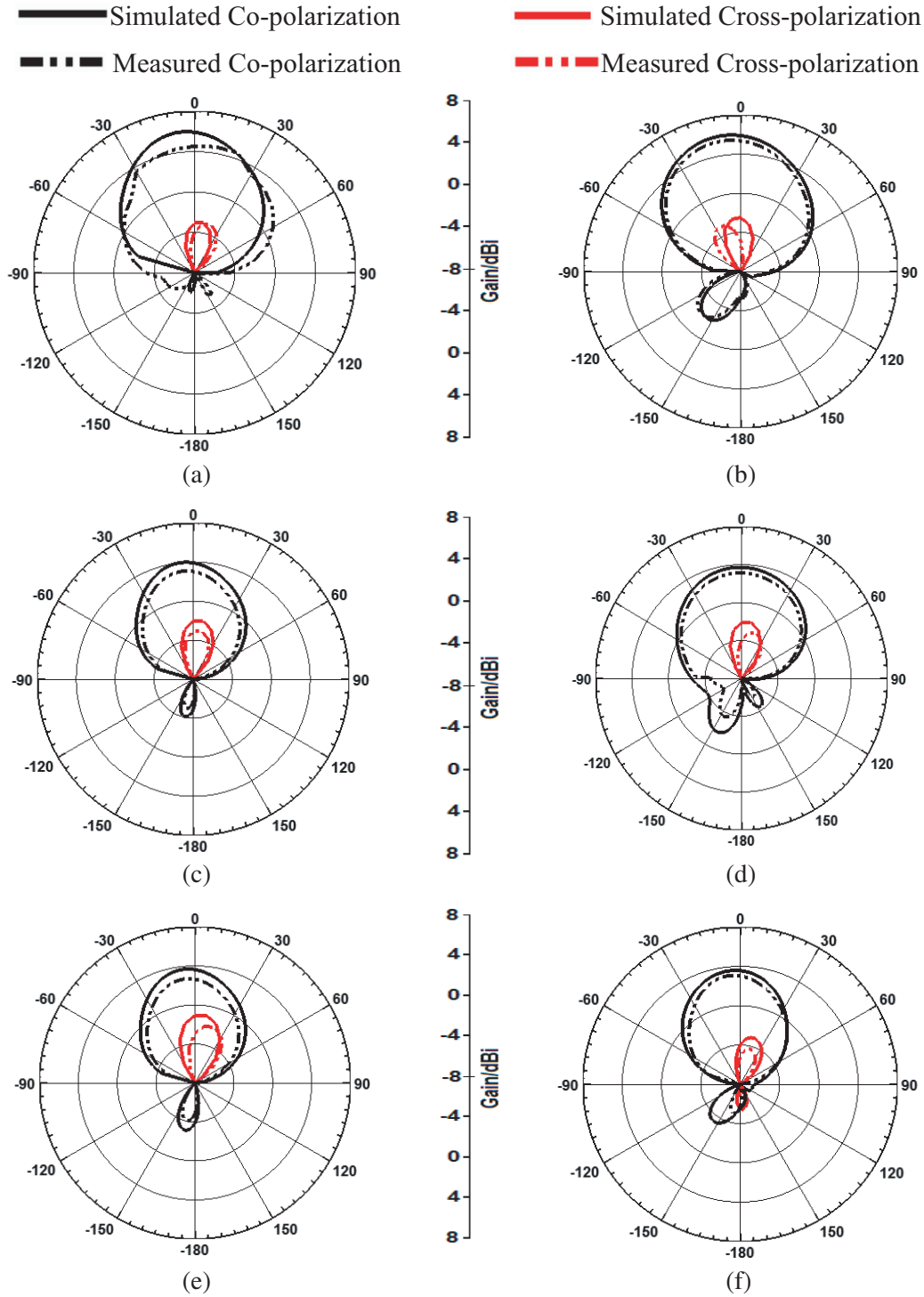


Figure 9. Simulate and measured Co and Cross-polarization radiation patterns: (a) *E*-plane at 12.25 GHz, (b) *H*-plane at 12.25 GHz, (c) *E*-plane at 14.16 GHz, (d) *H*-plane at 14.16 GHz, (e) *E*-plane at 17.50 GHz, (f) *H*-plane at 17.50 GHz.

The radiation efficiency (%) v/s frequency (GHz) plot is given in Fig. 11. It has been observed from Fig. 11 that the simulated values of the efficiency vary from 53 to 70%, 54 to 67%, and 67 to 69% at the frequency bands of 11.40–12.98 GHz, 14.21–14.86 GHz, and 17.41–18.98 GHz, respectively.

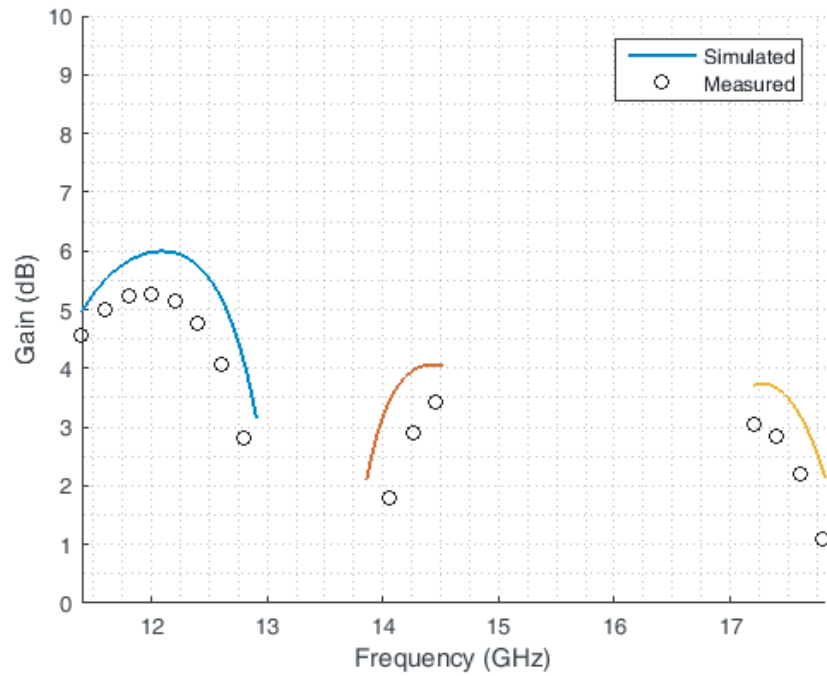


Figure 10. Gain (dBi) v/s frequency (GHz) plot.

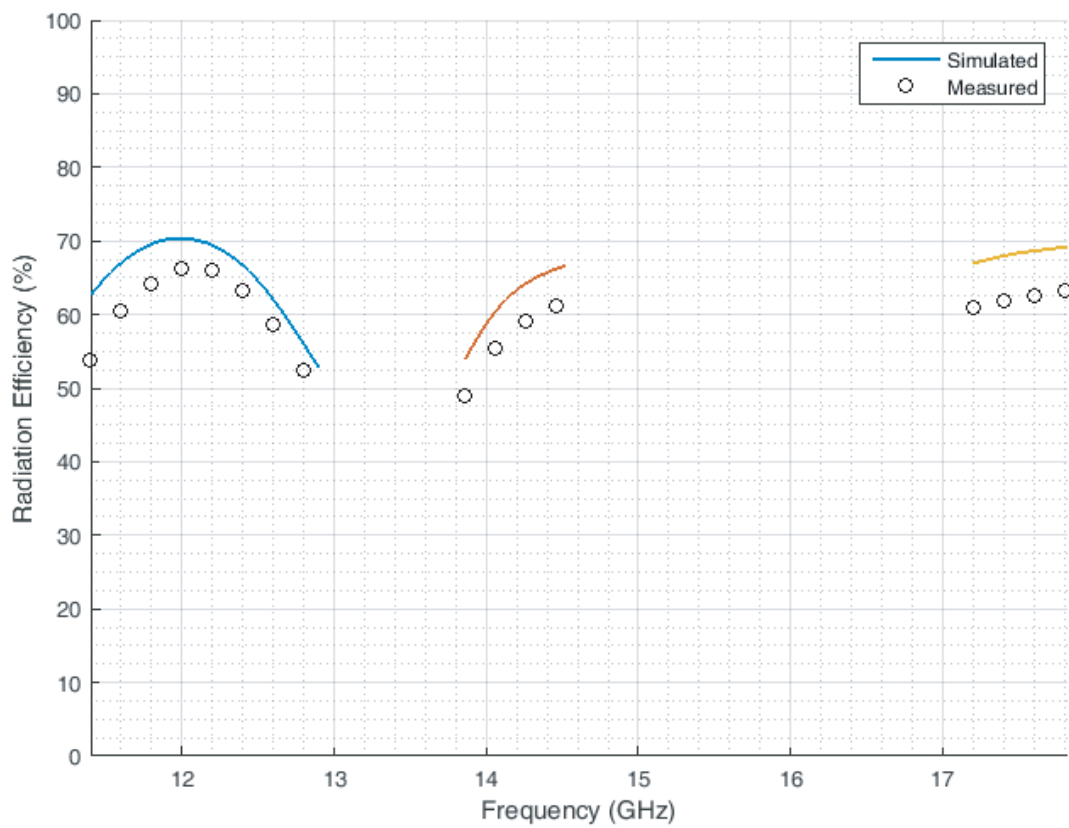


Figure 11. Radiation efficiency (%) v/s frequency (GHz) plot.

Conversely, the measured efficiency changes from 51 to 66%, 48 to 61%, and 61 to 64% at the frequency bands of 11.40–12.98 GHz, 14.21–14.86 GHz, and 17.41–18.98 GHz, respectively.

Table 3 gives the comparison of different antenna designs given in literature with the proposed design for the same application of interest. The proposed design achieves the three desired bands with the resonant frequencies of 12.25 GHz, 14.16 GHz, and 17.50 GHz with the percentage impedance bandwidths of 12.70%, 4.48%, and 8.63%, respectively. Moreover, the gain and efficiency are also found to be satisfactory.

Table 3. Proposed antenna design as compared to previous published designs. (RF: Resonant Frequency, BW: Bandwidth).

Design	RF of 1st Band (GHz)	RF of 2nd Band (GHz)	RF of 3rd Band (GHz)	BW of 1st Band	BW of 2nd Band	BW of 3rd Band	Patch size (mm ²)	Gain (dBi)	Efficiency (%)
Samsuzzaman et al. (2013) [15]	15.33	17.61	-	3.4	3.3	-	9.5 × 8	4.8–6.4	-
Vijayvergiya and Panigrahi (2017) [4]	12.07	14.44	-	10.2	8.2	-	10.1 × 9.9	4.8–7.4	68–78
Saini and Kumar (2019) [7]	12.38	14.40	-	12.29	9.37	-	10 × 10	1.6–4.2	69–80
Sayed et al. (2015) [10]	12.72	14.4	-	5.3	6.9	-	5.7 × 8	5–5.5	-
Thi et al. (2013) [12]	11.96	13.93	-	8.7	6.6	-	50 × 50	3.7–3.8	-
Parikh et al. (2012) [6]	11.95	14.25	-	4.2	3.6	-	9.4 × 7.1	5.7–7.2	-
Proposed	12.25	14.16	17.50	12.70	4.48	8.63	10 × 10	2.08–6	53 to 70

5. CONCLUSION

In this work, a low profile, small size tri-band antenna has been designed and fabricated for Ku band applications. The frequency bands required for the transmission and reception of DBS and FSS have been achieved using the proposed design. For this task, a truncated E-shaped slot, eight rectangular slots, two C-shaped slots in the patch, and eight defected ground structure (DGS) slots have been utilized. The results of the proposed antenna design are verified by comparing them with fabricated antenna results. Certain key parameters for satellite antennas like reflection coefficient, impedance bandwidth, polarization, efficiency, gain, and radiation pattern are taken for this analysis. The antenna design presented in this manuscript lays the ground work for array antennas. It can be used as an element in an array configuration to achieve enhanced gain suitable for transmission and reception modes of FSS and DBS which can be taken as a future endeavor for this study. This gain can be further enhanced using more refined material like RT Duroid substrate in future studies. Also, the proposed antenna fulfills the spectrum necessity of ITU region 3.

REFERENCES

1. Wong, K. L., *Compact and Broadband Microstrip Antennas*, Vol. 168, John Wiley & Sons, 2004.
2. Kumar, G. and K. Ray, *Broadband Microstrip Antennas*, Artech House, 2002.
3. James, J. R. and P. S. Hall, *Handbook of Microstrip Antennas*, 28, IET, 1989.
4. Vijayvergiya, P. L. and R. K. Panigrahi, "Single-layer single-patch dual band antenna for satellite applications," *IET Microwaves, Antennas and Propagation*, Vol. 11, No. 5, 664–669, 2016.
5. Kouhalvandi, L., S. Paker, and H. B. Yagci, "Ku-band slotted rectangular patch array antenna design," *2015 23th IEEE Signal Processing and Communications Applications Conf. (SIU)*, 447–450, 2015.
6. Parikh, H., S. V. Pandey, and M. Sahoo, "Design of a modified E-shaped dual band patchantenna for Ku band application," *Proceedings International Conference on Communication Systems and Network Technologies, CSNT*, 49–52, Rajkot, India, 2012.
7. Saini, G. S. and R. Kumar, "A low profile patch antenna for Ku-band applications," *International Journal of Electronics Letters*, 1–11, 2019.
8. Dubey, S. K., S. K. Pathak, and K. K. Modh, "High gain multiple resonance Ku band microstrip patch antenna," *IEEE Applied Electromagnetics Conf. (AEMC)*, 1–3, 2011.
9. Prasad, P. C. and N. Chattoraj, "Design of compact ku band microstrip antenna for satellite communication," *2013 Int. Conf. Communications and Signal Processing (ICCP)*, 196–200, 2013.
10. Sayed, A., R. S. Ghonam, and A. Zekry, "Design of a compact dual band microstrip antenna for Ku-band applications," *International Journal of Computer Applications*, Vol. 115, No. 13, 11–14, 2015.
11. Mao, Y., S. Guo, and M. Chen, "Compact dual-band monopole antenna with defected ground plane for Internet of things," *IET Microwaves, Antennas & Propagation*, Vol. 12, No. 8, 1332–1338, 2018.
12. Nguyen Thi, T., K. C. Hwang, and H. B. Kim, "Dual-band circularly-polarised Spidron fractal microstrip patch antenna for Ku-band satellite communication applications," *Electronics Letters*, Vol. 49, No. 7, 444–445, 2013.
13. Khare, A. and R. Nema, "Triple band parasitic array antenna for C-X-Ku-band application using out-of-phase coupling approach," *International Journal of Antennas and Propagation*, 2014.
14. Mathew, S., R. Anitha, U. Deepak, C. K. Aanandan, P. Mohanan, and K. Vasudevan, "A compact tri-band dual-polarized corner-truncated sectoral patch antenna," *IEEE Transactions on Antennas and Propagation*, Vol. 63, No. 12, 5842–5845, 2015.
15. Samsuzzaman, M., M. T. Islam, N. Misran, and M. M. Ali, "Dual band X shape microstrip patch antenna for satellite applications," *Procedia Technology*, Vol. 11, 1223–1228, 2013.
16. Naghar, A., O. Aghzout, M. Essaaidi, A. Alejos, M. Sanchez, and F. Falcone, "Ultra wideband and tri-band antennas for satellite applications at C-, X-, and Ku bands," *Proceedings of 2014 Mediterranean Microwave Symposium (MMS2014)*, 1–5, IEEE, December 2014.
17. Dhakad, S. K. and T. Bhandari, "A hexagonal broadband compact microstrip monopole antenna for C band, X band and Ku band applications," *2017 International Conference on Computing, Communication and Automation (ICCCA)*, 1532–1536, IEEE, May 2017.
18. Baudha, S. and V. Dinesh Kumar, "Corner truncated broadband patch antenna with circular slots," *Microwave and Optical Technology Letters*, Vol. 57, No. 4, 845–849, 2015.
19. Gupta, A., H. D. Joshi, and R. Khanna, "An X-shaped fractal antenna with DGS for multiband applications," *International Journal of Microwave and Wireless Technologies*, Vol. 9, No. 5, 1075–1083, 2017.
20. Nguyen Thi, T., K. C. Hwang, and H. B. Kim, "Dual-band circularly-polarised Spidron fractal microstrip patch antenna for Ku-band satellite communication applications," *Electronics Letters*, Vol. 49, No. 7, 444–445, 2013.
21. Lai, H. W., D. Xue, H. Wong, K. K. So, and X. Y. Zhang, "Broadband circularly polarized patch antenna arrays with multiple-layers structure," *IEEE Antennas and Wireless Propagation Letters*, Vol. 16, 525–528, 2016.

22. Deng, R., S. Xu, F. Yang, and M. Li, "A single-layer high-efficiency wideband reflectarray using hybrid design approach," *IEEE Antennas and Wireless Propagation Letters*, Vol. 16, 884–887, 2016.
23. Huang, J., W. Lin, F. Qiu, C. Jiang, D. Lei, and Y. Jay Guo, "A low profile, ultra-lightweight, high efficient circularly-polarized antenna array for Ku band satellite applications," *IEEE Access*, Vol. 5, 18356–18365, 2017.
24. Darimireddy, N. K., R. R. Reddy, and A. M. Prasad, "A miniaturized hexagonal-triangular fractal antenna for wide-band applications [Antenna Applications Corner]," *IEEE Antennas and Propagation Magazine*, Vol. 60, No. 2, 104–110, 2018.
25. Jang, H. K., J. H. Shin, and C. G. Kim, "Low RCS patch array antenna with electromagnetic bandgap using a conducting polymer," *IEEE International Conference in Electromagnetics Advance Applications*, 140143, Sydney, Australia, 2010.
26. Dhawan Singh and Viranjay M. Srivastava, "Comparative analyses for RCS of patch antenna using shorted stubs metamaterial absorber," *Journal of Engineering Science and Technology (JESTEC)*, Vol. 13, No. 11, 3532–3546, November 2018.
27. Balanis, C. A., *Antenna Theory: Analysis and Design*, 3rd Edition, John Wiley and Sons Inc, New York, 2005.